Supporting Information

Li et al. 10.1073/pnas.1213515110

SI Materials and Methods

Cells, Reagents, and Plasmids. Huh-7.5 cells (obtained from Charles Rice, The Rockefeller University, New York, NY) and FT3-7 cells were maintained as described previously (1, 2). PSI-6130 (β-D-2′-deoxy-2′-fluoro-2′-C-methylcytidine) (3) was the gift of Angela Lam and Phil Furman (Pharmasset, Princeton, NJ). WST-1 reagent (Millipore) was used to monitor cell viability using the manufacturer's protocol. Plasmids pH77S.3/*Gaussia princeps* luciferase (GLuc)2A, pH77S/GLuc2A-AAG, pH77S/AAG, pHJ3-5, pHJ3-5/GLuc2A, and the related S1-S2-p6m mutants have been described previously (1, 2, 4). pHJ3-5/NS5A$_{YFP}$ is a related plasmid in which the enhanced yellow fluorescent protein (EYFP) sequence has been fused in-frame within the carboxyl-terminal region of the NS5A protein-coding sequence (5). Plasmids expressing shRNAs against Rrp41, PM/Scl-100, or a control shRNA were kindly provided by William Marzluff (University of North Carolina at Chapel Hill, Chapel Hill, NC).

RNA Transcription. Viral RNAs were transcribed in vitro, and a nonmethylated 5′ guanosine cap was added where indicated, as described previously (4).

Transfections. siRNA pools targeting Xrn1, Upf1, or PM/Scl-100 and control siRNA pools (Dharmacon) were transfected using siLentfect Lipid Reagent (Bio-Rad). MicroRNA (miRNA) duplexes (50 nM) were transfected using siLentfect Lipid Reagent (Bio-Rad) where indicated. Lentiviral particles expressing shRNA against Rrp41 and PM/Scl-100 were produced using MISSION Lentiviral Packaging Mix (Sigma-Aldrich) and transduced into HeLa cells. Cells stably expressing shRNAs were selected by puromycin (4 μg/mL) for 7 d. In vitro–transcribed hepatitis C virus (HCV) RNA (1.25 μg) was transfected into 2.5×10^6 Huh-7.5 cells using the TransIT-mRNA Transfection kit (Mirus Bio).

Viral RNA Stability in Transfected Cells. RNA was transcribed in vitro from pH77S/GLuc2A-AAG, which contains the complete genotype 1a HCV sequence with GLuc2A placed in-frame within the polyprotein-coding region and a lethal GDD to AAG mutation in NS5B. Viral RNA (10 μg) and miRNA duplexes (4) (1 μM) were mixed with 1×10^7 HeLa cells in a 4-mm cuvettete and pulsed once at 300 V, 500 μF, and ∞ Ω in a Gene Pulser Xcell Total System (Bio-Rad). Cells were washed twice with PBS and plated in six-well plates. Total RNA was harvested at intervals, and HCV RNA abundance was measured by qRT-PCR. The percentage of RNA remaining at each time point was calculated with reference to that present immediately after transfection (0 h).

RNA Stability in HeLa S10 Lysate. HeLa S10 lysate was prepared as previously described except for the deletion of RNase treatment (6, 7). Lysate (10 μL) was mixed with duplex miRNAs (1 μM) in 20 μL reaction buffer (20 mM Hepes, pH 7.4, 40 mM potassium acetate, 1 mM ATP, 0.25 mM GTP, 25 mM creatine phosphate, 0.03 U/μL creatine phosphokinase) and incubated at 25 °C for 20 min. In vitro transcribed H77S RNAs (500 ng) were then added into the reaction mixtures. The reactions were stopped at the indicated time by adding 350 μL RNeasy Lysis Buffer (RNeasy Mini Kit; Qiagen) for RNA isolation. Five microliters of RNA was incubated with 2 μL SYTO 62 dye (1:1,000 dilution; Invitrogen) for 5 min at room temperature and then resolved by electrophoresis through a 1% Tris Borate EDTA-agarose gel and visualized, and fluorescent intensity was quantified using the Odyssey Infrared Imaging System.

Quantitative Real-Time RT-PCR. To quantify HCV RNA, cDNA was produced by reverse transcription of RNA using oligo(dT) and an HCV-specific primer (5′-GGCCAGTATCAGCACTCTCTGCA GTC-3′) targeting the 3′ UTR of the genome and SuperScript III Reverse Transcriptase (Invitrogen). qPCR analysis was carried out using iTaq SYBR Green Supermix with the CFX96 System (Bio-Rad). HCV RNA abundance was determined by reference to a standard curve using PCR primers targeting the 5′ UTR (5′-catggcgttagtatgagtgtcgt-3′ and 5′-ccctatcaggcagtaccacaa-3′), and normalized to the abundance of β-actin mRNA (primers: 5′-gtcaccggagtccatcacg-3′ and 5′-gacccagatcatgtttgagacc-3′).

Immunoblots. Immunoblotting was carried out using standard methods with the following antibodies: mouse mAb to β-actin (AC-74; Sigma-Aldrich), rabbit polyclonal antibody to Xrn1 (Bethyl Laboratory), mAb to HCV core protein (Pierce), and antibodies to Rrp41, PM/Scl-100, and Upf1 provided by William Marzluff. Protein bands were visualized with an Odyssey Infrared Imaging System (Li-Cor Biosciences).

Gaussia Luciferase Assay. Cell culture supernatant fluids were collected at intervals following RNA transfection, and cells were refed with fresh media. Secreted GLuc activity was measured using the Biolux Gaussia Luciferase assay kit (New England Biolabs) as previously described (4).

HCV RNA FISH and Confocal Fluorescence Microscopy. HCV RNA FISH was carried out using the QuantiGene viewRNA ISH Cell Assay Kit (Affymetrix) with an H77S-specific probe set (Affymetrix viewRNA probe set VF1-11279) following the manufacturer's instructions. Following the FISH protocol, P bodies were stained with rabbit polyclonal antibody to Xrn1 (Bethyl Laboratory) or a mouse monoclonal antibody specific for Dcp1a (Abnova) and Alexa-488–conjugated goat anti-rabbit or mouse antibody (Invitrogen). For visualization of HCV replication complexes, we monitored intrinsic NS5A-EYFP fluorescence in cells transfected with synthetic HJ3-5/NS5A$_{YFP}$ RNA. Where indicated, nuclei were counterstained with DAPI. Laser scanning confocal microscopy was carried out using an Olympus FV1000 Multiphoton Confocal Microscope within the Michael Hooker Microscopy Facility of the University of North Carolina (Chapel Hill, NC).

Semiautomatic analysis of digitally recorded images including a quantitative pixel analysis of the colocalization of Xrn1 and HCV RNA was accomplished using MetaMorph 7.1 software (Molecular Devices). To quantify overlap between the RNA signal and Xrn1 in P bodies, we selectively analyzed large Xrn1-positive structures setting the threshold value to exclude cytosolic Xrn1 signals. Similarly, we quantified HCV RNA colocalization with Xrn1 in the cytoplasm using the appropriate threshold values. The overlap of HCV RNA signals with cytosolic Xrn1 was calculated by subtracting HCV RNA localizing to P bodies from that overlapped with cytoplasmic Xrn1.

Infectious Virus Titration. Supernatant fluids (100 μL) from H77S-transfected cells were incubated with 5×10^4 Huh-7.5 cells in a 48-well plate for 6 h. Media were changed, and cells were allowed to grow for 72 h before staining with anti-core antibody (Pierce). Foci of infected cells were visualized and infectious virus titer quantified in terms of focus-forming units (FFUs) as described (8).

Circularization RT-PCR. Total RNA (10 μg) from Huh-7 cells infected with HJ3-5 virus were incubated with or without RNA polyphosphatase (Epicentre Biotechnologies) in a 20-μL reaction

for 0.5 h at 37 °C following the manufacturer's recommended procedures. The RNA was then extracted with phenol-chloroform, precipitated with ethanol, and resuspended in 10 μL H_2O. Circularization of RNA was performed in a 20-μL reaction containing 10 U of T4 RNA ligase (New England Biolabs) overnight at 16 °C. The samples were extracted and precipitated as above. Ligation products were reverse transcribed with SuperScript III Reverse Transcriptase (Invitrogen) using an RT primer specific for HCV (5′-gcgcgacctacgccgggggt-3′). Two microliters of the product were used in 50 μL PCR with Platinum Taq Polymerase (Invitrogen). Primers 1 and 2 (5′ tggctccatcttagccctagtcacg-3′ and 5′-gttccgcagaccactatggctc-3′) (Fig. S2*A*) were used to amplify regions in the 3′ and 5′ UTR of HCV RNA in the ligated product. A 20-μL aliquot of each reaction was analyzed by electrophoresis through a 1.8% (wt/vol) agarose gel. PCR bands were excised from the gel, purified, cloned using the TOPO TA Cloning Kit (Invitrogen), and sequenced.

Polysome Profiling. Huh-7.5 cells (2×10^7) were electroporated with 40 μg of HJ3-5 or HJ3-5 S1-S2p6m RNA and incubated at 37 °C. Six hours later, cycloheximide was added to the medium to a final concentration of 250 μM, and the cells were incubated for an additional 15 min. Cells were then harvested and lysed in lysis buffer [20 mM Tris-HCl, pH 7.5, 150 mM KCl, 10 mM $MgCl_2$, 1 mM DTT, 500 μM cycloheximide, 1% Nonidet P-40, 0.5% deoxycholate, protease inhibitor (Roche), and 50 U/mL RNaseOUT (Invitrogen)] for 15 min. The lysate was centrifuged at 9,500 × *g* for 10 min, and the supernatant was loaded onto a 10–50% (wt/vol) sucrose gradient. The gradient was centrifuged at 160,000 × *g* for 5 h, and 400- to 500-μL fractions were collected. RNAs in each fraction were purified using TRIzol LS reagent (Invitrogen) following the manufacturer's instructions and subjected to agarose gel electrophoresis and HCV- and actin-specific real-time RT-PCR.

Statistical Methods. qRT-PCR data from RNA decay experiments were fit to a one-phase decay model, and decay constants were compared using the extra sum-of-squares *F*-test. All statistical tests were run using GraphPad by Prism, Version 5.0c.

1. Shimakami T, et al. (2012) Base pairing between hepatitis C virus RNA and microRNA 122 3′ of its seed sequence is essential for genome stabilization and production of infectious virus. *J Virol* 86(13):7372–7383.
2. Jangra RK, Yi M, Lemon SM (2010) miR-122 regulation of hepatitis C virus translation and infectious virus production. *J Virol* 84:6615–6625.
3. Stuyver LJ, et al. (2006) Inhibition of hepatitis C replicon RNA synthesis by β-D-2′-deoxy-2′-fluoro-2′-C-methylcytidine: a specific inhibitor of hepatitis C virus replication. *Antivir Chem Chemother* 17(2):79–87.
4. Shimakami T, et al. (2012) Stabilization of hepatitis C virus RNA by an Ago2-miR-122 complex. *Proc Natl Acad Sci USA* 109(3):941–946.
5. Ma Y, et al. (2011) Hepatitis C virus NS2 protein serves as a scaffold for virus assembly by interacting with both structural and nonstructural proteins. *J Virol* 85(1):86–97.
6. Murray KE, Roberts AW, Barton DJ (2001) Poly(rC) binding proteins mediate poliovirus mRNA stability. *RNA* 7(8):1126–1141.
7. Barton DJ, Morasco BJ, Flanegan JB (1996) Assays for poliovirus polymerase, 3D (Pol), and authentic RNA replication in HeLa S10 extracts. *Methods Enzymol* 275: 35–57.
8. Yi M, Villanueva RA, Thomas DL, Wakita T, Lemon SM (2006) Production of infectious genotype 1a hepatitis C virus (Hutchinson strain) in cultured human hepatoma cells. *Proc Natl Acad Sci USA* 103(7):2310–2315.

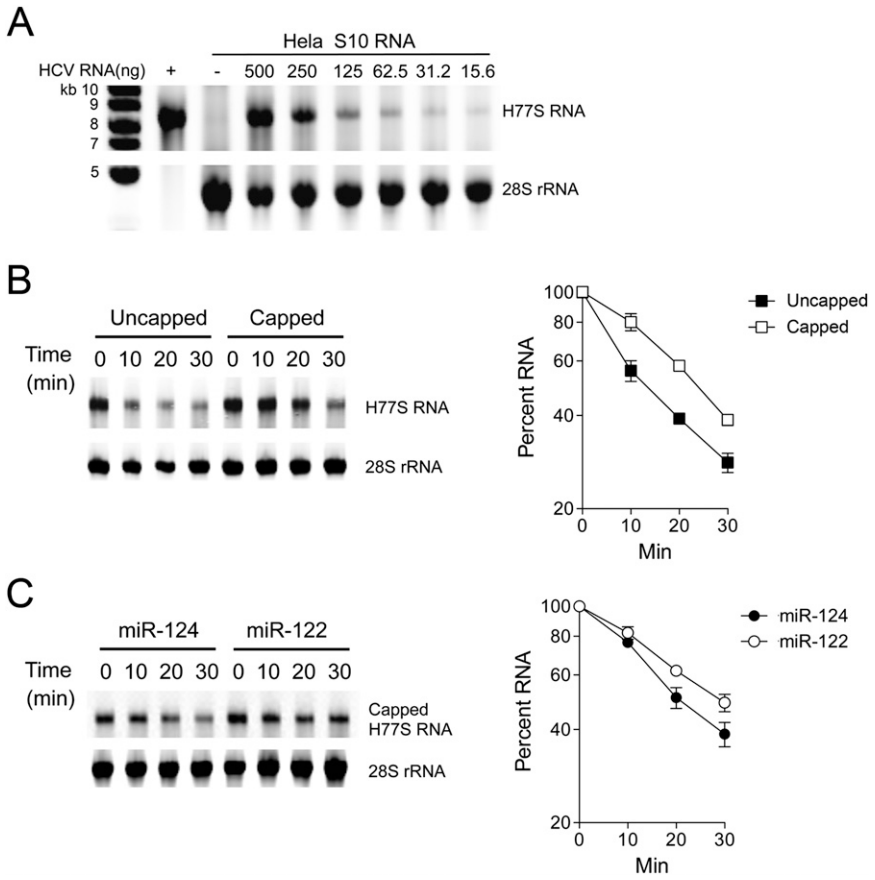

Fig. S1. Stability of HCV RNA in HeLa S10 lysate. (*A*) Sensitivity of SYTO 62 staining. Total RNA extracted from 50 μg HeLa S10 lysate was mixed with the indicated amount of synthetic in vitro–transcribed HCV RNA (H77S), incubated with SYTO 62 for 5 min, and resolved on a 1% TBE-agarose gel. (*B*) Capped and uncapped H77S RNAs were incubated with HeLa S10 lysate, extracted at indicated time intervals, stained with SYTO 62, and resolved in 1% agarose. Percent HCV RNA remaining was quantified relative to 28S rRNA. Results are the means of three experiments ± SEM. (*C*) Capped H77S RNA was incubated with HeLa S10 lysate containing the indicated miRNA (1 μM). RNAs were extracted and quantified as in *B*.

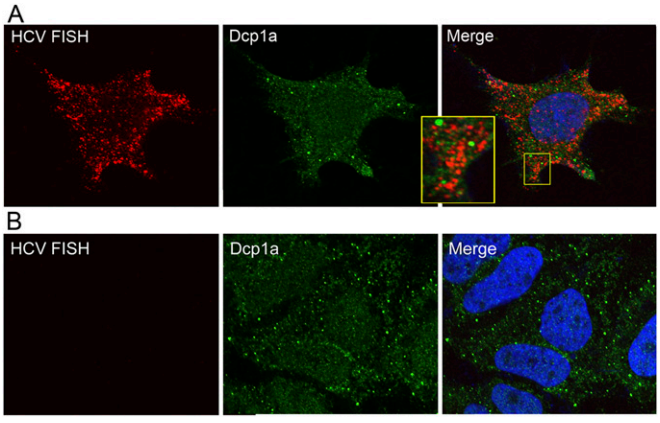

Fig. S2. Confocal microscopy demonstrating the absence of association of HCV RNA with Dcp1a, a marker of P bodies. Huh-7.5 cells were (*A*) transfected with H77S.3 RNA for 4 d, or (*B*) mock-transfected, and then subjected to FISH for detection of HCV RNA (red). P bodies were visualized by subsequent immunostaining for Dcp1a (green). Nuclei in the merged image were visualized by DAPI counterstain. *Inset* represents an enlarged view of a portion of the merged image.

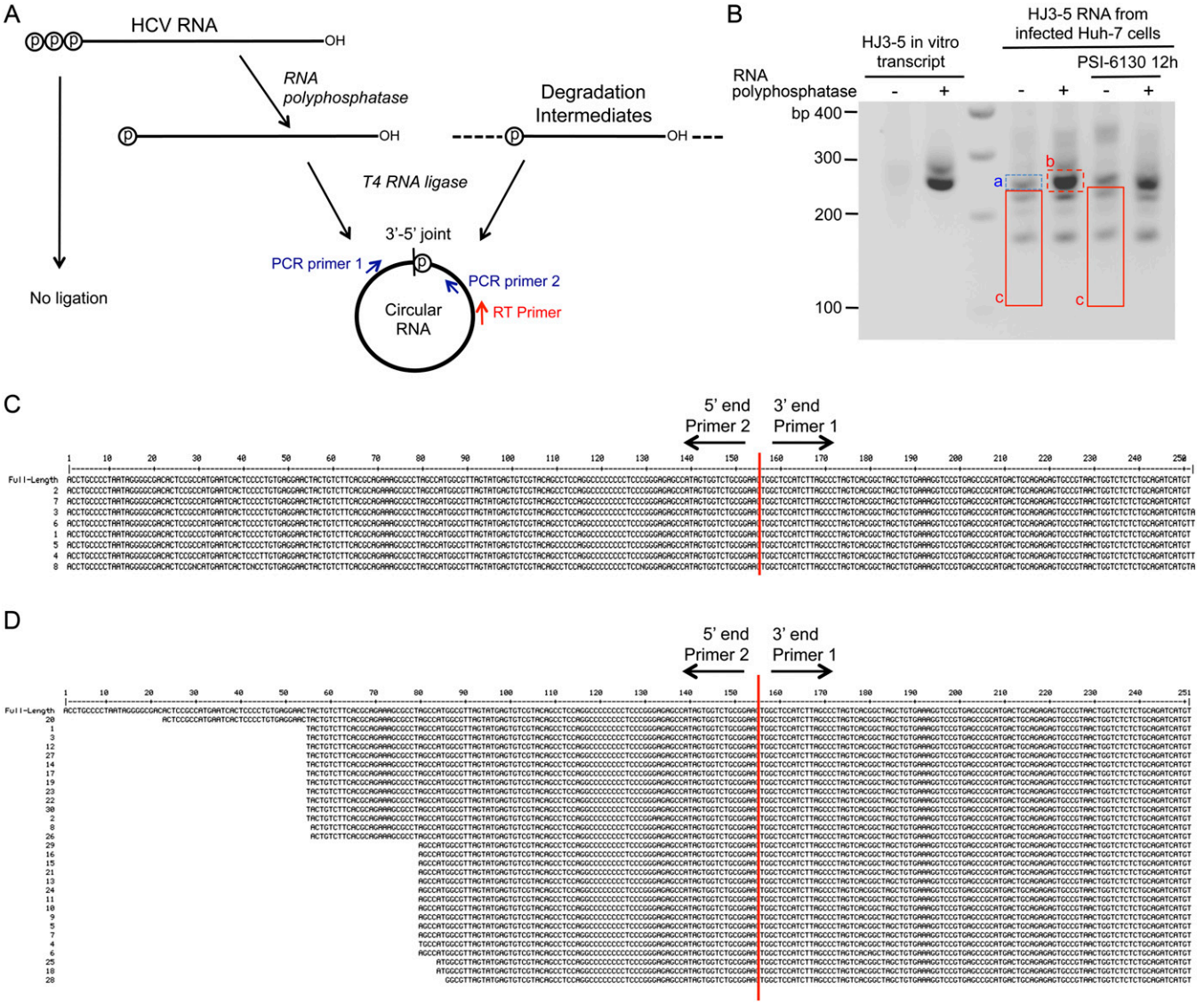

Fig. S3. Identification of HCV RNA degradation intermediates by circularization RT-PCR (cRT-PCR). (*A*) cRT-PCR strategy used to define the 5′ and 3′ ends of intact HCV viral RNA and its degradation intermediates. (*B*) Products of cRT-PCR reactions using total RNA extracted from Huh-7 cells infected with HJ3-5 virus (with or without PSI-6130 treatment), either pretreated or not pretreated with RNA polyphosphatase to remove 5′ triphosphates. Products were separated in 1.8% agarose gels, and different regions excised from the gel, cloned, and sequenced. Synthetic HJ3-5 RNA was used as a positive control. Band a (dashed blue box) represents nonspecific amplification of ribosomal RNA. (*C*) Sequences of multiple clones from band b (dashed red box in *B*, primarily full-length HCV RNA, detected only after RNA polyphosphatase treatment) were aligned with the full-length HCV RNA 5′ and 3′ end sequences. (*D*) Sequences of multiple clones from region c (solid red box in *B*, degradation products) were aligned as in *D*.

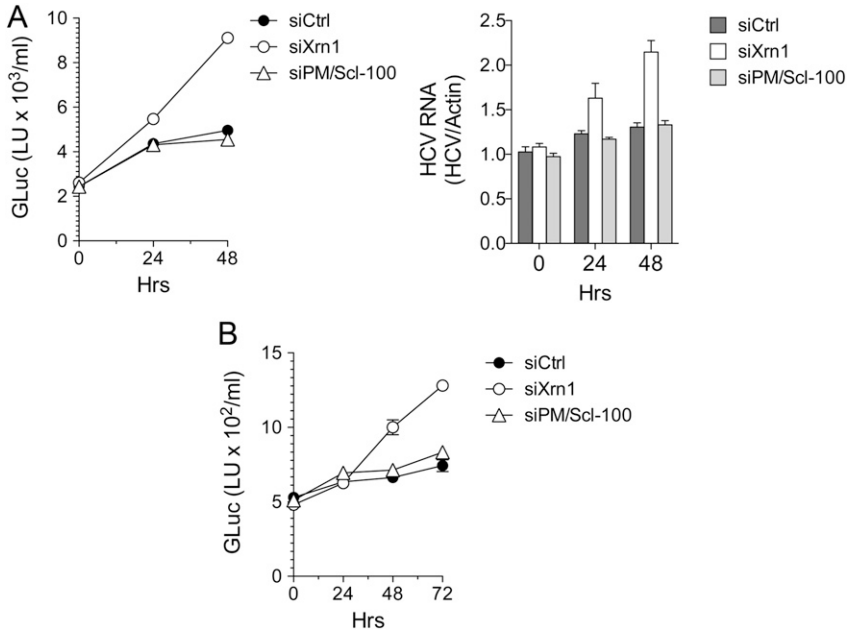

Fig. S4. Impact of Xrn1 knockdown in established HCV infection. (*A*) (*Left*) Huh-7.5 cells transfected with genotype 1a H77S/GLuc RNA 5 d previously were retransfected with siRNAs against Xrn1 or PM/Scl-100 or scrambled control siRNA (siCtrl). GLuc activities were measured at 0, 24, and 48 h later. Significant increases in GLuc activity were observed in Xrn1 knockdown cells at 24 and 48 h posttransfection. (*Right*) Cells were collected and total RNA extracted. HCV RNA levels were determined by qRT-PCR relative to β-actin mRNA abundance. (*B*) FT_3-7 cells infected with the chimeric HCV HJ3-5/GLuc2A virus were transfected with siRNA specific for Xrn1, PM/Scl-100, or control siCtrl siRNA. GLuc activities were measured at 0, 24, 48, and 72 h following siRNA transfection. Significant increases in GLuc activity were observed in Xrn1 knockdown cells at 48 and 72 h posttransfection.

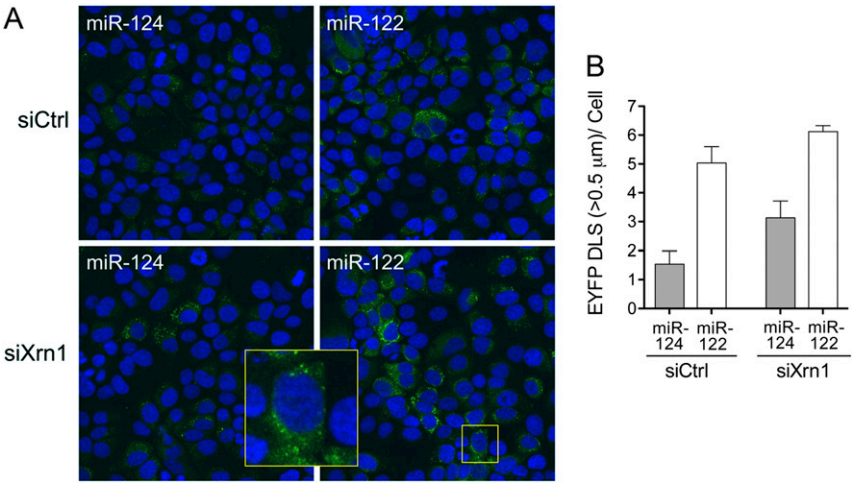

Fig. S5. miR-122 supplementation enhances formation of large, NS5A-containing dot-like structures (DLS) in Xrn1-depleted cells. (*A*) Confocal microscopy images of NS5A-EYFP fluorescence in Huh-7 cells supporting replication of HJ3-5/$NS5A_{YFP}$ RNA. Cells were transfected with siCtrl or siXrn1, and then 48 h later retransfected with these siRNAs and either miR-122 or miR-124. NS5A-EYFP fluorescence was assessed 24 h after miRNA supplementation. (*B*) Mean numbers of large (>0.5 μm diameter) DLS per cell in multiple microscopic fields determined by semiautomatic image analysis.

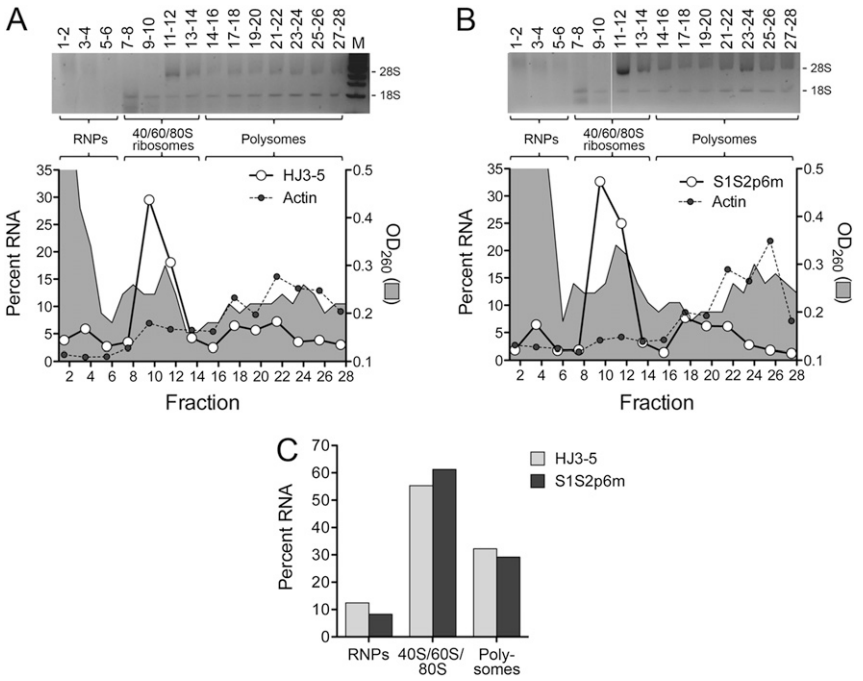

Fig. S6. Polysome analysis of cells transfected with HJ3-5 HCV RNA and the related miR-122 binding mutant, HJ3-5/S1-S2p6m. (*A*) HJ3-5 and (*B*) HJ3-5/S1-S2p6m RNA were electroporated into Huh-7.5 cells. Cells were harvested 6 h later, and lysates were subjected to rate-zonal centrifugation on a 10–50% sucrose gradient. Fractions (400–500 μL each) were collected, and RNAs were extracted. (*Upper*) 28S and 18S ribosome RNAs were resolved by electrophoresis in a 1% agarose gel. (*Lower*) HCV and β-actin RNA in each fraction was quantified by real-time RT-PCR, and the percentage of total HCV or β-actin RNA in each fraction was plotted, together with the OD_{260} of each fraction. (*C*) Percentage of total HJ3-5 and HJ3-5/S1-S2p6m RNAs associated with ribonucleoproteins (RNPs) (fractions 1–6), 40/60/80S ribosomes (fractions 7–14), and polysomes (fractions 15–28).

Table S1. Estimated $t_{1/2}$ of transfected nonreplicating HCV RNA in HeLa cells following RNAi-mediated knockdown of 5′ exonuclease and exosome proteins

	No miR-122 supplementation			With miR-122 supplementation		
Manipulation	$t_{1/2}$ (h)	95% CI	R^2	$t_{1/2}$ (h)	95% CI	R^2
siCtrl	1.38	1.10–1.89	0.9639	2.31	1.76–3.30	0.8176
siXrn1	3.21	2.41–4.79	0.7369	4.93	3.80–7.00	0.7001
siUpf1	1.69	1.37–2.00	0.9355	2.69	2.00–4.16	0.7453
shCtrl	2.13	1.85–2.52	0.9642	2.90	2.30–3.71	0.8947
shPM/Scl-100	4.45	3.89–5.25	0.9405	7.16	6.01–8.86	0.8191
shRrp41	3.57	3.08–4.24	0.9889	4.82	3.91–6.31	0.8499

Table S2. Estimated $t_{1/2}$ of H77S vs. H77S/S1-S2p6m RNA in HeLa S10 lysate

	H77S RNA			H77S/S1-S2p6m RNA		
miRNA	$t_{1/2}$ (min)	95% CI	R^2	$t_{1/2}$ (min)	95% CI	R^2
No miRNA	18.6	16.4–21.7	0.9388	15.7	14.5–17.0	0.9642
miR-124	21.1	19.1–23.8	0.9621		ND	
miR-122	39.0	34.9–44.1	0.9429	18.2	15.6–21.9	0.9207
miR-122p6		ND		35.37	31.3–40.7	0.9435

ND, not determined.

Table S3. Estimated $t_{1/2}$ of H77S RNA in S10 lysate from Xrn1 and exosome knockdown cells

Manipulation	$t_{1/2}$ (min)	95% CI	R^2
siCtrl	12.0	10.6–13.7	0.9822
siXrn1	14.7	13.4–16.3	0.9875
shCtrl	12.4	11.0–14.2	0.9674
shPM/Scl-100	25.4	22.8–28.6	0.9584
shRrp41	19.3	17.6–21.5	0.9716